

Simultaneous Conventional and Plenoptic Background Oriented Schlieren Imaging

Jenna N. Klemkowsky^{1,*}, Christopher J. Clifford¹, Brian S. Thurow¹, Brett F. Bathe²

¹: Dept. of Aerospace Engineering, Auburn University, Auburn, AL, USA

²: NASA Langley Research Center, Advanced Measurement and Data Systems Branch, Hampton, VA, USA

* Correspondent author: jenna.klemkowsky@auburn.edu

Keywords: plenoptic imaging, background oriented schlieren, plenoptic BOS

HIGHLIGHTS

- Conventional and plenoptic BOS simultaneously acquired measurements of a laminar plume using three different focal plane configurations.
- Conventional BOS results in a single line-of-sight measurement with high spatial resolution.
- Plenoptic BOS results in multiple line-of-sight measurements at a lower resolution compared to conventional BOS.
- Both systems provide results that support the well-known sensitivity trend observed in BOS experiments.
- Results of this work have led to proposed explanations and have raised additional questions that require further exploration.

ABSTRACT

Plenoptic Background Oriented Schlieren (BOS) is an emerging schlieren technique that is capable of providing 3D qualitative and quantitative information about density gradients present in a wide range of fluid dynamics problems. In this work, the fundamental concepts of plenoptic BOS are reviewed before discussing an open-air experiment with a buoyant plume where both conventional BOS and plenoptic BOS measurements were acquired simultaneously. Both cameras had the same field-of-view for all experiments, and three different focal plane arrangements were explored: (1) the focal plane was set to the background positions and the plume varied between 11 different positions relative to this focal plane, (2) the focal plane was set to 635-millimeters in front of the background position, and (3) the nominal focal plane varied while the position of the plume remained fixed. Such discussion will provide insight on how the two techniques compare, and what additional work is required to better understand the results provided by these two imaging systems.

Simultaneous Conventional and Plenoptic Background Oriented Schlieren Imaging

Jenna N. Klemkowsky^{1,*}, Christopher J. Clifford¹, Brian S. Thurow¹, Brett F. Bathel²

1: Dept. of Aerospace Engineering, Auburn University, Auburn, AL, USA

2: NASA Langley Research Center, Advanced Measurement and Data Systems Branch, Hampton, VA, USA

* Correspondent author: jenna.klemkowsky@auburn.edu

Keywords: plenoptic imaging, background oriented schlieren, plenoptic BOS

ABSTRACT

Plenoptic Background Oriented Schlieren (BOS) is an emerging schlieren technique that is capable of providing 3D qualitative and quantitative information about density gradients present in a wide range of fluid dynamics problems. In this work, the fundamental concepts of plenoptic BOS are reviewed before discussing an open-air experiment with a buoyant plume where both conventional BOS and plenoptic BOS measurements were acquired simultaneously. Both cameras had the same field-of-view for all experiments, and three different focal plane arrangements were explored: (1) the focal plane was set to the background positions and the plume varied between 11 different positions relative to this focal plane, (2) the focal plane was set to 635-millimeters in front of the background position, and (3) the nominal focal plane varied while the position of the plume remained fixed. Such discussion will provide insight on how the two techniques compare, and what additional work is required to better understand the results provided by these two imaging systems.

1. Introduction

The collection of schlieren techniques provides a way to obtain density measurements in transparent media. Such measurements are obtained through density's relationship with refractive index, commonly known as the Gladstone-Dale relation for gaseous media. Due to most flows being inherently three-dimensional, numerous efforts have been made within the last decade towards 3D schlieren measurements. Typically these 3D approaches require either a multi-camera configuration (Atcheson et al., 2008; Goldhahn & Seume, 2007; Nicolas et al., 2016) or the rotation of the object generating density gradients (Ota, Hamada, Kato, & Maeno, 2011; Venkatakrisnan & Meier, 2004).

Recently, an alternative 3D approach was introduced to the collection of schlieren techniques called plenoptic background oriented schlieren, or plenoptic BOS (Klemkowsky, Fahringer, Clifford, Bathel, & Thurow, 2017). This technique provides the ability to collect 3D information from a single imaging system called the plenoptic camera. It has potential to provide an easy-to-

use, robust setup compared to the current 3D systems, particularly for experiments possessing limited optical access. In this work, we present recent progress in the development of plenoptic BOS particularly in how this technique compares to the commonly used conventional BOS technique. Using a buoyant thermal plume to produce density gradients, conventional BOS and plenoptic BOS measurements were acquired simultaneously. Three different configurations were setup in order to explore the sensitivity of the plenoptic BOS system in an open-air test environment. This experiment highlights some of the benefits and limitations of each imaging system, which is important particularly in showcasing the capabilities of the plenoptic BOS technique.

2. Plenoptic Background Oriented Schlieren Imaging

BOS was first introduced to the scientific community in the late 1990s by two different research groups, one of which called it ‘synthetic schlieren’ (Dalziel, Hughes, & Sutherland, 1998, 2000; Meier, 1999). A random patterned background, placed behind the object producing density gradients (referred to hereafter as the schlieren object), is imaged with and without the presence of such gradients. Through image processing algorithms such as cross-correlation or optical flow, a vector displacement field is obtained by observing an apparent shift in the pattern caused by the density gradients present in the scene. Each measured displacement is dependent upon a line-of-sight integration, where its magnitude depends on both the strength of the refractive index gradients and their position within the experimental setup. BOS with a single conventional camera typically provides qualitative 2D information, which leaves any three-dimensionality ambiguous.

The concept of the plenoptic camera was first introduced by Adelson and Wang (Adelson & Wang, 1992) and was further developed by Ng et al. (Ng et al., 2005) for handheld photography. The plenoptic camera is capable of sampling the 4D light field – a term used to define the distribution of light rays in terms of spatial and angular coordinates. This capability is provided by the insertion of a microlens array at the image plane, where each microlens focuses the incident light onto pixels behind it. The angle at which the incident light propagates determines which pixel is illuminated behind a certain microlens. When acquiring a single image with this system, each microlens represents the spatial position of a given light ray while each pixel represents the angle of propagation of that same light ray.

In the post-processing period, a single raw plenoptic image can be used to render images from multiple viewing positions (multiple perspectives) and from different synthetic focal planes. The

plenoptic cameras used throughout this paper were constructed by the Advanced Flow Diagnostics Laboratory (AFDL) at Auburn University. The base camera was a 29 megapixel IMPERX Bobcat 2.0 B6620 CCD camera, which contains a 471×362 hexagonally arranged microlens array inserted approximately $308 \mu\text{m}$ in front of the image sensor. Each microlens has a pitch of $77 \mu\text{m}$, and each pixel on the image sensor has a pitch of $5.5 \mu\text{m}$.

The plenoptic BOS technique (Klemkowsky, Fahringer, Clifford, et al., 2017) provides an approach that exploits the capabilities of the plenoptic camera while using the same concepts of a conventional BOS system. Raw plenoptic images are acquired with and without the presence of the schlieren object. Each raw image is processed to generate multiple perspective views, where a specific perspective view rendered with and without the presence of the schlieren object is classified as an image pair. Through image processing algorithms such as cross-correlation, image displacements are obtained per image pair. A single image pair from plenoptic BOS is analogous to a conventional BOS image pair except at a lower spatial resolution (a result of sub-sampling pixels behind the microlens array to generate each perspective view). Using the displacements determined from each image pair, the 4D BOS displacement field is created. This is comparable to the 4D scalar intensity field captured in the raw plenoptic images, except the BOS displacement field is a 4D vector field. Structuring the data in this manner provides the ability to exploit the refocusing capabilities of light field photography. This results in the ability to generate 'focused BOS' images, where density gradients will come into and out of focus when changing the synthetic focal plane within the volume.

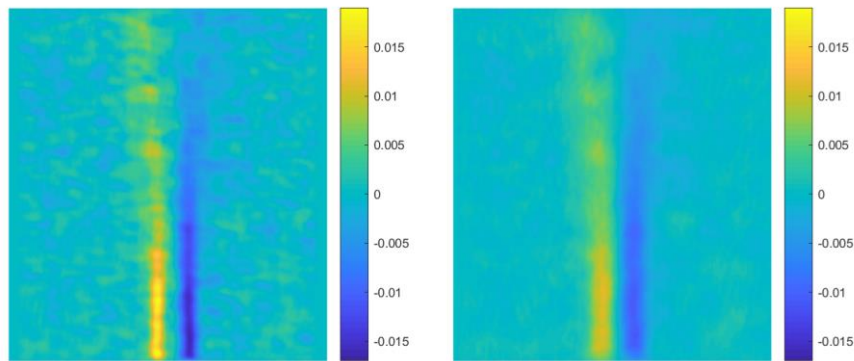


Fig. 1 Focused BOS images rendered at a synthetic focal plane near the plume position (left) versus far away (right).

An example of this is shown in Fig. 1, where a single laminar plume was used as the schlieren object. Qualitative observations show that when focused BOS images are generated at various synthetic focal planes, the location at which the schlieren object occurs where the signature of the

density gradients are most in-focus. Fig. 1 shows this in-focus location (left) compared to a synthetic plane that produces an out-of-focus signature (right). Additional steps have been taken to quantify the schlieren object position by computing spatial gradients across each focused BOS images. From the gradient image, a single spatially-averaged gradient value is obtained for each synthetic focal plane image. The peak spatially-averaged gradient value is then assumed to correspond to the point with which the synthetic focal plane is aligned with the schlieren object. This method, while simple in nature, has initially provided success in quantifying the position of density gradients in 3D space.

3. Experimental Configuration

Experiments were performed in the Advanced Measurement and Data Systems Branch at NASA Langley Research Center. A buoyant thermal plume was produced using a series of electrically resistive heating elements that collect room temperature air through an inlet port on the bottom, heat up the air inside a thermally insulated box, from which the air exits at an outlet port at the top. This box has an internal volume of 0.3 m × 0.3 m × 0.3 m, and it can accommodate different types of nozzles placed at the exit port. For these experiments, an aluminum tube with an inner diameter of approximately 25 mm was used in order to provide a laminar plume at an internal flow box temperature of 300-degrees Celsius. To limit the influence of room air currents, two Plexiglas windows were placed on the left and right sides of the field-of-view surrounding the plume.

These experiments, also used to preliminarily compare the two imaging systems (Klemkowsky, Fahringer, Thurow, & Bathel, 2017), used an AF DC-Nikkor 135 mm, f/2 main lens on both cameras. The background was printed on a 0.9 m × 0.9 m sheet of paper, which consisted of a wavelet pattern based on the work of Cook et al. (Cook & DeRose, 2005). The background was illuminated from behind using a combination of 20-watt, 30-watt, and 50-watt AmScope LED Cold Fiber Optic Illuminators.

The conventional BOS measurements were taken with a 29 megapixel IMPERX Bobcat 2.0 B6640 CCD camera. The sensors of the plenoptic camera and the conventional camera were nearly identical with the exception of their bit-depths which were 14-bit and 12-bit, respectively. The data from the 14-bit plenoptic camera was down-sampled to 12-bit prior to processing in order to compare image performance independent of bit-depth. During image acquisition, both cameras were adjusted such that their optical axes were collinear with the use of a 50/50 plate beam splitter.

Both cameras were also adjusted such that they had the same raw magnification (i.e. same field-of-view in the raw plenoptic and conventional images). As an additional step for the plenoptic imaging system, dot card images were also taken during each set of experiments in order to properly calibrate the volume over which BOS measurements were acquired. The dot card contained 6.35 mm dots with 12.7 mm spacing between dot centers. Volumetric calibration was performed according to Hall et al. (Hall, Fahringer, Guildenbecher, & Thurow, 2018).

During post processing, cross-correlation was performed on both conventional image pairs and rendered perspective view images pairs from the raw plenoptic images, where the perspective view image pairs were rendered at a resolution of 900x600. The implemented algorithm was developed by Fahringer et al. (Fahringer, Lynch, & Thurow, 2015). Cropping was performed on all image pairs (both conventional and plenoptic) to select the region in the field-of-view containing the background pattern without any obstructions, which varied for each plume position in both image types.

Cross-correlation was performed using 4 passes, where the final pass was 8x8 pixels with 50% overlap. For plenoptic BOS, there is the added step of rendering focused BOS images. All focused BOS images throughout the following sections were rendered by synthetically placing the focal plane at the known location of the plume within the volume. Each focused BOS image is rendered with a resolution that super-sampled the number of measured vectors by a factor of two. This resolution varies due to the cropped region used during cross-correlation.

Three different data sets were collected during this experiment: (1) the nominal focal plane was set on the background, (2) the nominal focal plane was set at a position of 635 mm in front of the background, and (3) the nominal focal plane varied while the position of the plume remained fixed. For data sets (1) and (2), the plume was placed at 11 different positions within the volume, where positions ranged from 381 to 1651 mm in front of the background. For Data Set (3), the plume was placed at 1524 mm from the background and the focal plane was moved to 6 different positions.

Table 1 shows the experimental parameters for BOS Data Set (1) and (2). The exposure for each camera was selected such that the distribution of intensities was centered about the midpoint of the camera's dynamic range. The depth-of-field (DOF) for each conventional setup was based on a circle of confusion of 10 pixels, which was determined to be approximately 1.2 meters and 0.75

meters, respectively. The DOF associated with a focused BOS image refocused to the position of the plume is shown for each of the 11 positions in Table 2. As the plume position moves farther from the background, the DOF for a focused BOS image decreases. This is a result of the increase in effective magnification at the desired synthetic focal plane. The purpose of displaying these values is to show their similarity to that of the conventional system. The conventional system uses a narrow aperture ($f/\#=16$) to achieve the mentioned DOF. A single perspective view rendered from a raw plenoptic image is similar to a pinhole aperture, thus providing a large DOF. Because a focused BOS image uses the full collection of perspective views, it effectively uses a full aperture which results in a DOF similar to that of the conventional system.

Table 1 Experimental parameters for BOS Data Sets (1) and (2).

	<i>BOS Data Set (1)</i>		<i>BOS Data Set (2)</i>	
	Plenoptic:	Conventional:	Plenoptic:	Conventional:
Magnification	-0.04	-0.04	-0.05	-0.05
f/#	~4	16	~4	16
Exposure (ms)	19	210	20.5	260

Table 2 DOF for each focused BOS image rendered at its respective plume position relative to the background position for BOS Data Sets (1) and (2).

Plume Position (mm):	Plenoptic BOS Data Set 1 (m)	Plenoptic BOS Data Set 2 (m)
362	1.8	1.37
508	1.73	1.31
635	1.65	1.26
762	1.58	1.2
889	1.51	1.14
1016	1.43	1.09
1143	1.36	1.03
1270	1.29	0.97
1397	1.22	0.92
1524	1.14	0.86
1651	1.07	0.81

As stated earlier for BOS Data Set (3), the focal plane position varied to 6 different positions while the plume was positioned at 1524 mm in front of the background. Similar fields-of-view were

maintained at each focal plane position. Tables 3 and 4 show the experimental parameters for each focal plane position in this data set. The DOF for the plenoptic images is the DOF of a focused BOS image at the location of the plume position, and the DOF of the conventional system was based on a circle of confusion of 10 pixels. It is important to note the similarity of DOF between these two image types though their $f/\#$ were rather different during data acquisition.

Table 3 Parameters for BOS Data Set (3) where the focal plane varied with respect to the background position.

	<i>Focal Plane Positions (measure relative to background position)</i>					
	0 mm		381 mm		762 mm	
	(background position)					
	<i>Plenoptic</i>	<i>Conventional</i>	<i>Plenoptic</i>	<i>Conventional</i>	<i>Plenoptic</i>	<i>Conventional</i>
Magnification	-0.04	-0.041	-0.047	-0.044	-0.053	-0.052
$f/\#$	4	16	4	16	4	16
Exposure (ms)	20.5	260	22	280	23	280
DOF (mm)	1142	1118	887	970	796	696

Table 4 Continuation of Table 3 with the three remaining focal plane positions.

	<i>Focal Plane Positions (measure relative to background position)</i>					
	1143 mm		1524 mm		1905 mm	
	<i>Plenoptic</i>	<i>Conventional</i>	<i>Plenoptic</i>	<i>Conventional</i>	<i>Plenoptic</i>	<i>Conventional</i>
Magnification	-0.063	-0.06	-0.076	-0.075	-0.096	-0.095
$f/\#$	4	16	4	16	4	16
Exposure (ms)	22	280	21	280	20	280
DOF (mm)	647	524	529	339	332	215

4. Results

To provide some consistency throughout this discussion, there are a few considerations to be made. All conventional and focused BOS images are an average of 24 instantaneous images taken during image acquisition for each data set. All images have been rendered such that their axes and measured displacements are in terms of millimeters in image space, the native domain of traditional BOS. Since the plume was placed in the vertical direction in the field-of-view, significant displacements occurred solely in the x-direction. The following results were rendered using only the measured x-displacements. All focused BOS images were rendered from a

collection of 113 unique perspective views. Each focused BOS image was then scaled such that the measured displacements correspond to their magnitude at the virtual image sensor position, as shown in Fig. 2. The resulting displacements are $d_{virtual} = (M_{virtual}/M_b) d$, where M_b the magnification at the wavelet background is, $M_{virtual}$ is the magnification at the synthetic focal plane, and d is the original displacement measurement corresponding to the background plane.

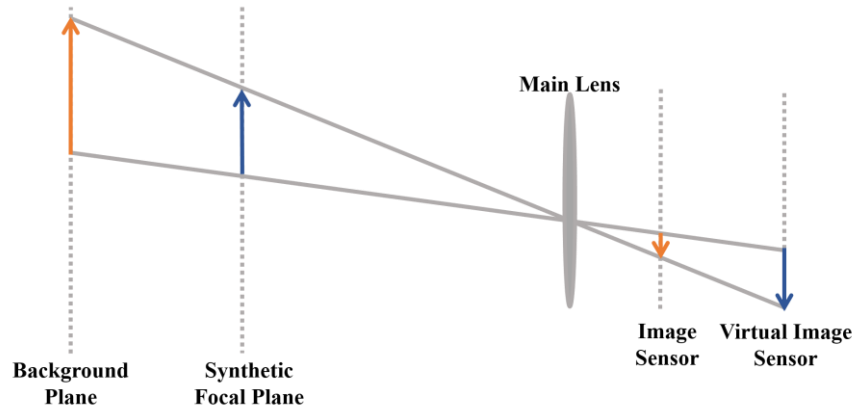


Fig. 2 Schematic of scaling displacements based on the desired synthetic focal plane and the corresponding virtual image sensor.

A. BOS Data Set (1) and BOS Data Set (2)

As an example of the qualitative differences between the two imaging systems, Fig. 3 shows conventional BOS (left), focused BOS (center), and center perspective BOS (right) measurements for the plume positioned at 1397 millimeters in front of the background. While the laminar structure of the plume is apparent in each of the figures, the most obvious differences can be observed between the conventional and center perspective BOS images. This is a result of spatial resolution, where the resolution of the conventional system is defined by the pixel size (0.0055 mm) compared to the perspective image being defined by the "effective" pixel size of one microlens (0.077mm). This is the trade-off of a plenoptic imaging system, where spatial resolution is sacrificed for additional angular information, from which depth resolution is gained.

Fig. 4 shows the maximum displacements measured from conventional BOS (red), center perspective BOS (black), and focused BOS (green) for each of the 11 different plume positions in BOS Data Set (1). The scatter points at each plume position represent the measurements obtained from 0.5 to 2 mm above the base of the plume. This region was selected because it provides the largest displacements and most discernable portion of the plume for all 11 positions. As a reminder, this data set placed the focal plane on the background position which is often the desired focal plane location in BOS literature. A few important observations can be made from Fig. 4. The

first corresponds to the sensitivity of the displacement measurements. In all three image types, as the plume position moves farther from the background, the maximum measured displacement increases. This is a well-known trend in BOS experiments, where it is ideal to have a large distance between the schlieren object and the background. The data presented here supports this trend for each image type.

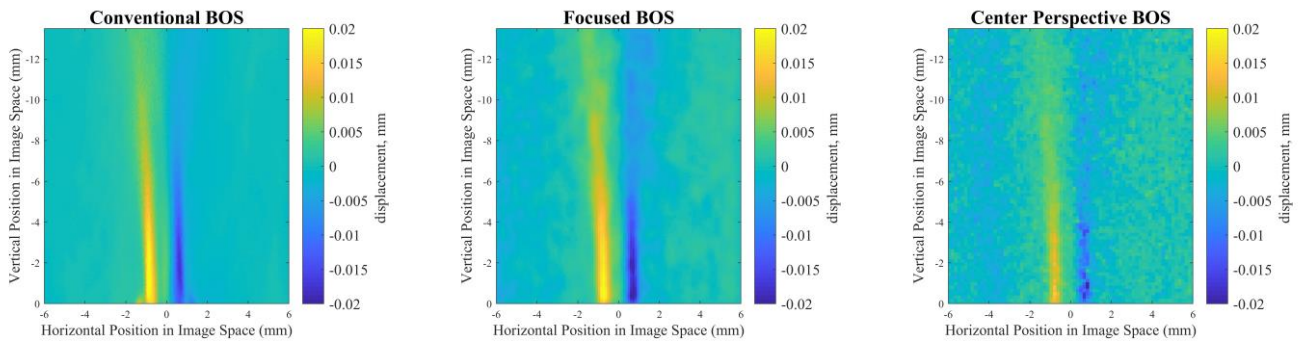


Fig. 3 Conventional BOS (left), focused BOS (center), and center perspective BOS (right) images of the plume positioned 1397 mm in front of the background.

Another observation made is with regards to measurements determined by the center perspective image pair. The authors hypothesized that the measurements determined by a center perspective view would result in the same measurements determined by the conventional system because they are a single line-of-sight measurement with the same field-of-view. According to the results in Fig. 4, this does not appear to be true. For each plume position, the maximum displacements from the center perspective view are always lower than that of the conventional. It appears that the center perspective observed maximum displacements that are approximately 50% of the maximum measured displacements of the conventional. It is proposed that this could be a result of several potential factors. The first is that with the decrease in spatial resolution in a single perspective image and with the limited frequency range available in the particular wavelet pattern used for these experiments, the background did not provide optimal detail for the rendered resolution. Another factor could be due to the hexagonal packing of the microlens array, where the light field data must be interpolated to obtain the appropriate irradiance value in a traditional rectilinear perspective image. Currently, a linear interpolation scheme is used, which might result in blurring the detail of the wavelet pattern. Future work is required to explore other potential interpolation methods and how their results compare to the results shown in Fig. 4.

Another interesting observation with respect to Fig. 4 is that the maximum displacements measured by focused BOS start to approach and then eventually surpass the maximum

displacements measured by conventional BOS. While the cause of this trend is currently unknown, the authors propose the following explanation. Both the conventional system and the center perspective view are a line-of-sight integrated 2D measurement. The sensitivity of their BOS measurements is a result of where the schlieren object is with respect to the background and the overall strength of the density gradients produced by the schlieren object. Because focused BOS images are rendered using a collection of angular information, not only is its sensitivity a result of the two items mentioned above, it is also sensitive to parallax. In this data set, as the plume moves farther from the background (the focal plane position), it simultaneously moves closer to the camera, thus increasing the available parallax. This results in an increase in the diversity of lines-of-sight capable of measuring the displacements caused by the presence of the plume. This compounding effect could explain why the focused BOS surpasses conventional BOS at the most sensitive plume position. This added sensitivity could result in focused BOS varying quadratically as a function of plume position compared to the other two image types only varying linearly. Additional experiments are required to verify this proposed reasoning and/or to observe if other factors including the current interpolation algorithms contribute to this observation.

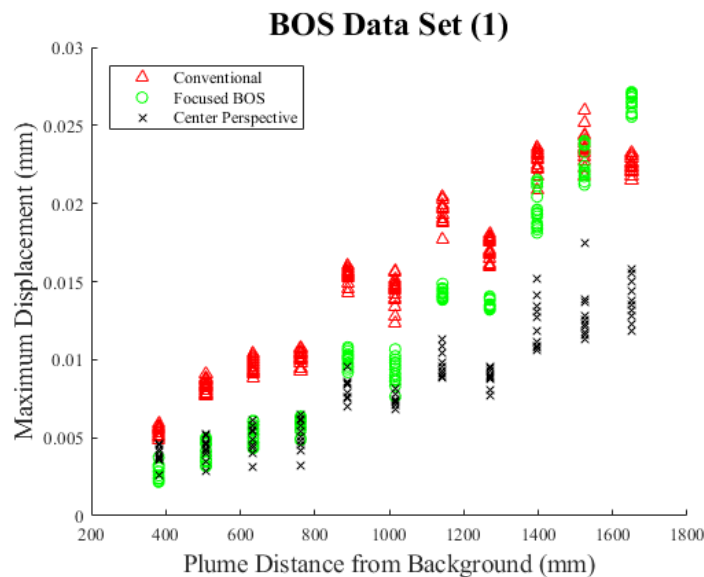


Fig. 4 BOS Data Set (1): Maximum measured displacement for each plume position with respect to the background position, where the scatter represents the measurements obtained from 0.5 to 2 mm above the base of the plume.

Unfortunately for BOS Data Set (2), dot card images were not taken throughout the entire volume rather they were only taken up to 1143 mm in front of the background. This means that plume positions beyond 1143 mm were not within the calibration scope and are thus not shown. Fig. 5 shows the maximum displacements measured from conventional BOS (red), center perspective

BOS (black), and focused BOS (green) for 7 calibrated plume positions in this data set. The scatter points at each plume position represent the measurements obtained from 0.5 to 2 mm above the base of the plume. These results are in good agreement with the observations already discussed with regards to Data Set (1) in Fig. 4, where the maximum displacement measured by each image type increases as the plume position moves farther from the background, and the maximum displacement measured by a center perspective is approximately 50% of the maximum displacement measured by the conventional system. Unfortunately, the observation that the maximum displacements of focused BOS surpasses that of the conventional BOS cannot be made due to the limitation created by the dot card calibration.

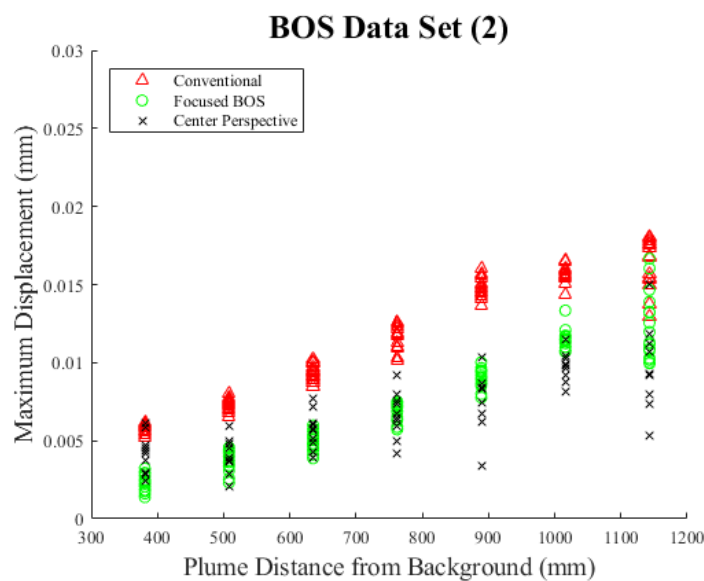


Fig. 5 BOS Data Set (2): Maximum measured displacement for each plume position with respect to the background position, where the scatter represents the measurements obtained from 0.5 to 2 mm above the base of the plume.

C. BOS Data Set (3)

BOS Data Set (3) was performed to explore the influence of the focal plane position on the measured displacements. It was expected that this variation would change the magnitude of measured displacement because the selection of a focal plane position defines several experimental parameters including magnification, DOF, and the optimal placement of the schlieren object and the background. For this data set, the background and the plume remained at a fixed position. Fig. 6 shows the measured maximum displacement of the plume for each of the 6 focal plane positions for conventional BOS (red), center perspective BOS (black), and focused BOS (green). The scatter points represent a height of 0.5 to 2 mm above the base of the plume. Note that when the focal plane is set on the background, the results provided in this data set are

comparable to the results shown in BOS Data Set (1) when the plume is positioned at the same location (1524 mm).

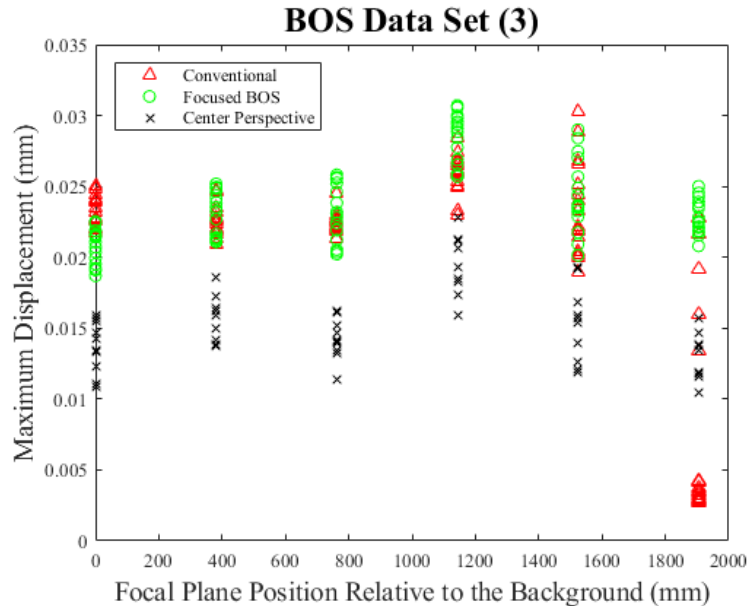


Fig. 6 BOS Data Set (3): Maximum measured displacement with respect to each focal plane position, where the scatter represents the measurements obtained from 0.5 to 2 mm above the base of the plume

Over the range of focal planes selected, it appears that the maximum measured displacement does not significantly change for each of the three image types. There is a decrease in the measurement for conventional BOS at the focal plane farthest from the background, where the magnification is increased. This is a result of the background being too far outside of the DOF resulting in loss of detail in the background pattern. If this were a required configuration for a BOS experiment, the background could be optimized such that a larger range of frequencies are available in the wavelet pattern. This decrease in measurement is likely for the perspective and focused BOS images, but is not shown over this range of focal plane positions. This is due to the larger DOF available in a perspective view, which is used in both the measurements for a single perspective and a focused BOS image. A larger DOF results in the ability for detail in the background to be captured over a larger depth range. This is also represented in the previous data sets, where the maximum displacements are similar in magnitude for each of the plume positions for the two different focal plane positions. The authors do not suggest that a change in focal plane position will always result in a consistent maximum displacement rather this is purely a result of the experimental parameters used in this study including the length scale of the setup and the consistent strength of the laminar plume.

It can also be observed that as the focal plane moves closer to the camera, the maximum measured displacements from focused BOS result in similar or slightly larger results than that of conventional BOS. As the focal plane moves closer to the camera, the amount of available parallax decreases at the plume position but increases at the background position. Alongside the increase in magnification which results in measurements available over a larger portion of the field-of-view, this influence of parallax could be an additional contributing factor. This observation supports the proposed explanation mentioned with regards to BOS Data Set (1) where the larger parallax provides increased sensitivity to the focused BOS results. As stated before, additional experiments are required to verify the proposed reasoning.

5. Conclusions and Future Work

With plenoptic BOS being relatively new to the scientific community, it is important to make comparisons with traditional methods currently being used in experimental facilities. In this work, conventional BOS and plenoptic BOS measurements were acquired simultaneously of a laminar buoyant thermal plume using three different focal plane variations. Several observations were made with respect to results from conventional BOS, focused BOS, and center perspective BOS. In support of the known sensitivity of a BOS configuration, all three image types provided results that show the maximum measured displacement increases as the distance between the background and the plume increased. Also, with respect to qualitative observations, the plenoptic system suffers from a decrease in spatial information in order to acquire multiple line-of-sight measurements in a single snap shot. Though not shown in this work, this addition of angular information allows focused BOS images to quantify the position of the plume in 3D space.

These data sets have also led to posing several unanswered questions. Is there an added increase in sensitivity due to an increase in parallax in focused BOS? If parallax contributes to the sensitivity of the focused BOS system, what does the trend look like compared to that of the conventional BOS system? These first two questions will be answered with an experiment that holds the plume-to-background distance and focal plane location constant, while varying the plume-to-camera distance. Also, does a change in interpolation scheme when rendering perspective views improve the measurements determined from cross-correlation? Do the measurements become comparable to the results of conventional BOS? The use of a higher-order interpolation, such as the sinc function which preserves high-frequency content, may be better suited. In addition, when varying the focal plane position, what is the limit for the plenoptic system? How does this limit rely on or influence the other parameters in the experiment? Future

experiments are required to answer these questions, and such work will result in an even better understanding of how these two imaging systems compare.

Acknowledgements

The assistance of Mr. Stephen Jones of the Advanced Measurement and Data Systems Branch at the NASA Langley Research Center is acknowledged for his assistance in setting up the BOS measurement system. In addition, the first author was funded by the Alabama Space Grant Consortium (ASGC), NASA Training Grant #NNX15AJ18H. The authors would like to acknowledge the support of the Transformational Tools and Technologies (TTT) and Aeronautics Evaluation and Test Capabilities (AETC) projects for their support of this work.

References

- Adelson, E. H., & Wang, J. (1992). Single Lens Stereo with a Plenoptic Camera. *IEEE Transactions on Pattern Analysis and Machine Intelligence*, 14(2), 99–106. <https://doi.org/10.1109/34.121783>
- Atcheson, B., Ihrke, I., Heidrich, W., Tevs, A., Bradley, D., Magnor, M., & Seidel, H. (2008). Time-resolved 3D Capture of Non-stationary Gas Flows. *ACM Transactions on Graphics*, 27(5), 1. <https://doi.org/10.1145/1409060.1409085>
- Clifford, C. J., Klemkowsky, J. N., Thurow, B. S., Arora, N., & Alvi, F. S. (2017). Visualization of an SBLI using Plenoptic BOS. *55th AIAA Aerospace Sciences Meeting*, (January), 1–10. <https://doi.org/10.2514/6.2017-1643>
- Cook, R. L., & DeRose, T. (2005). *Wavelet Noise*. Association for Computing Machinery. <https://doi.org/10.1145/1073204.1073264>
- Dalziel, S. B., Hughes, G. O., & Sutherland, B. R. (1998). Synthetic Schlieren. *Proceedings of the 8th International Symposium on Flow Visualization*.
- Dalziel, S. B., Hughes, G. O., & Sutherland, B. R. (2000). Whole-field density measurements by “synthetic schlieren.” *Experiments in Fluids*, 28(4), 322–335. <https://doi.org/10.1007/s003480050391>
- Fahringer, T. W., Lynch, K. P., & Thurow, B. (2015). Volumetric particle image velocimetry with a single plenoptic camera. *Measurement Science and Technology*, 26. <https://doi.org/10.1088/0957-0233/26/11/115201>
- Goldhahn, E., & Seume, J. (2007). The background oriented schlieren technique: Sensitivity, accuracy, resolution and application to a three-dimensional density field. *Experiments in Fluids*, 43, 241–249. <https://doi.org/10.1007/s00348-007-0331-1>
- Hall, E. M., Fahringer, T. W., Guildenbecher, D. R., & Thurow, B. S. (2018). Volumetric calibration of a plenoptic camera. *Applied Optics*, 57(4), 914. <https://doi.org/10.1364/AO.57.000914>
- Klemkowsky, J. N., Fahringer, T. W., Clifford, C. J., Bathel, B. F., & Thurow, B. S. (2017). Plenoptic Background Oriented Schlieren Imaging. *Measurement Science and Technology*, (28). <https://doi.org/10.1088/1361-6501/aa7f3d>
- Klemkowsky, J. N., Fahringer, T. W., Thurow, B. S., & Bathel, B. F. (2017). Preliminary Comparison Between Conventional and Plenoptic Background Oriented Schlieren Imaging.

33rd AIAA Aerodynamic Measurement Technology and Ground Testing Conference, (June).

<https://doi.org/10.2514/6.2017-4067>

Meier, G. E. A. (1999). Hintergrund Schlierenmessverfahren. *Deutsche Patentanmeldung*, (DE 199 42 856 A1).

Ng, R., Levoy, M., Brédif, M., Duval, G., Horowitz, M., & Hanrahan, P. (2005). *Light Field Photography with a Hand-Held Plenoptic Camera*. <https://doi.org/10.1.1.163.488>

Nicolas, F., Micheli, F., Donjat, D., Plyer, A., Champagnat, F., & Le Besnerais, G. (2016). 3D reconstruction of compressible flow by synchronized multi camera BOS. In *18th International Symposium on the Application of Laser and Imaging Techniques to Fluid Mechanics*. Lisbon, Portugal.

Ota, M., Hamada, K., Kato, H., & Maeno, K. (2011). Computed-tomographic density measurement of supersonic flow field by colored-grid background oriented schlieren (CGBOS) technique. *Measurement Science and Technology*, 22(10).

<https://doi.org/10.1088/0957-0233/22/10/104011>

Venkatakrishnan, L., & Meier, G. E. A. (2004). Density measurements using the Background Oriented Schlieren technique. *Experiments in Fluids*, 37, 237–247.

<https://doi.org/10.1007/s00348-004-0807-1>